Available online at BCREC website: https://bcrec.id

Bulletin of Chemical Reaction Engineering & Catalysis, 18 (1) 2023, 162-172

Research Article

Effect of Additional Polyethylene Glycol and Citric Acid on Characteristics of NiMo/γ-Al_2O_3 Catalyst in Light Cycle Gas Oil Hydrodesulfurisation

Dede Sukandar[1*], Lailatul Badriyah[1], Wawan Rustyawan[2], Adawiah Adawiah[3*]

[1]Department of Chemistry, Faculty of Science and Technology, UIN Syarif Hidayatullah Jakarta, Jl. Ir. H. Juanda No. 95, Ciputat, Tangerang Selatan 15412, Indonesia.
[2]Catalyst And Materials, Research and Technology Innovation (RTI), Direktorat SPPU, PT Pertamina (Persero), Jalan Raya Bekasi Km 20, Pulogadung, Jakarta
[3]Integrated Laboratory Centre, Faculty of Science and Technology, UIN Syarif Hidayatullah Jakarta, Jl. Ir. H. Juanda No. 95, Ciputat, Tangerang Selatan 15412, Indonesia

Received: 4th January 2023; Revised: 16th April 2023; Accepted: 17th April 2023
Available online: 18th April 2023; Published regularly: April 2023

Abstract

Sulfur is an impurity in diesel that causes low product quality and environmental pollution. Therefore, a catalyst is needed in the profound hydrodesulfurization (HDS) reaction to produce diesel fuel with low sulfur content. The catalyst synthesized in this work was NiMo/γ-Al_2O_3 with the addition of PEG (2%, 4%, 6%) (w/w) and CA (1%, 2%, and 4%) (w/w). The catalyst was synthesized using the dry impregnation method with a metal concentration of 3% NiO and 15% MoO_3. The obtained catalysts were characterized using X-Ray Fluorescence (XRF), X-Ray Diffraction (XRD), and Surface Area Analyzer (SAA). This work acquired the best catalyst characteristics for the HDS process by adding 2% PEG and 1% CA with a concentration of 3.19% NiO and 13.98% MoO_3. The surface area, pore volume, and diameter are 181.655 m^2/g, 0.50 cm^3/g, and 110.51 Å, respectively. The catalyst activity satisfies Euro V standards at 345 °C with a sulfur content of 9.55 ppm, and the sulfur conversion (HDS) is 98.75%. The density and cetane index of the obtained diesel fuel was 0.798 g/mL and 53.6, respectively.

Keywords: PEG; Polyethylene Glycol; Citric Acid; Hydrodesulfurization; NiMo/γ-Al2O3; Light Cycle Gas Oil

How to Cite: D. Sukandar, L. Badriyah, W. Rustyawan, A. Adawiah (2023). Effect of Additional Polyethylene Glycol and Citric Acid on Characteristics of NiMo/γ-Al_2O_3 Catalyst in Light Cycle Gas Oil Hydrodesulfurisation. *Bulletin of Chemical Reaction Engineering & Catalysis*, 18(1), 162-172 (doi: 10.9767/bcrec.17036)

Permalink/DOI: https://doi.org/10.9767/bcrec.17036

1. Introduction

Diesel petroleum is fuel in all diesel engines with high rotation above 1000 rpm [1]. The sulfur content represents the quality of diesel petroleum in vehicle exhaust emissions. The sulfur content in diesel fuel will produce sulfur dioxide (SO_2) gas emissions which harm health, because it causes respiratory problems and headaches and can attack human nerves [2,3]. The sulfur content in diesel fuel also triggers ex-

* Corresponding Author.
Email: sukandarkimia@uinjkt.ac.id (D. Sukandar)

cess acid levels, damaging pipes, pumps, and distillation equipment used in automotive engines. The crust in the fuel line can interfere with the supply of fuel flowing into the cylinder. This results in the incomplete combustion of diesel engine fuel and decreased engine power [4]. In addition, the sulfur component in fuel is poisonous to the catalyst [5,6].

Fuel quality in Indonesia tends to move towards Ultra Low Sulfur Diesel (ULSD), which is <10 ppm or the total elimination of sulfur content in diesel fuel [7]. It relates to efforts to protect the environment in legislation regarding the content of impurities in vehicle exhaust gases [8]. The maximum boundary for sulfur specified in Indonesian diesel fuel specifications according to the Directorate General of Oil and Gas No. 28.K/10/DJM.T/2016 is 0.005% m/m or the equivalent of 50 ppm.

Hydrodesulfurization (HDS) is a process of removing sulfur impurities contained in petroleum fractions during processing. HDS requires relatively high temperatures and pressures, namely at 300-350 °C and 50-100 atm [9]. Multifarious catalysts have been widely used to accelerate the hydrodesulfurization rate, such as NiMo/γ-Al_2O_3 and CoMo/γ-Al_2O_3 [10-13]. The NiMo/γ-Al_2O_3 catalyst has high stability and is not poisoned, so it can be used for a long time [14]. Steiner reported that the NiMo/γ-Al_2O_3 catalyst provided HDS catalytic activity and better resistance to sulfur poisoning than CoMo/γ-Al_2O_3 [13]. Topsoe *et al.* added that the NiMo/γ-Al_2O_3 catalyst could carry out hydrodesulfurization and hydrodenitrogenation reactions resulting in a more excellent conversion than CoMo/γ-Al_2O_3 [15]. Kamalia stated that the NiMo/γ-Al_2O_3 catalyst could reduce the sulfur content in kerosene to 1.84 ppm with a conversion of 99.5% at 345 °C [16]. Wang *et al.* also conveyed that the NiMo/γ-Al_2O_3 catalyst can reduce the sulfur content in shale oil to 2600 ppm with a conversion of 80.7% at 380 °C [17].

The NiMo/γ-Al_2O_3 catalyst has a unique composition: mesoporous alumina is the support, and NiMo is the active metal. Al_2O_3 is desirable alumina in hydrotreating industrial applications because it has a large surface area of about 250-350 m^2/g [18]. The surface area of alumina is a wildly determining parameter in the dispersion of Ni and Mo oxides because the dispersion of Mo becomes higher when the surface area of alumina is enormous. However, the catalyst's active sites can be damaged, or its activity decreases if the catalyst surface is coated with metal (poisoning). Limited interaction between metal and support can lead to uneven distribution of active metal and accumulation of active components on the support surface [19]. Therefore, additives are needed to control the interaction of active metal components and support during the catalyst synthesis process.

Sorts of additives that can be added are polyethylene glycol (PEG) and Citric Acid (CA) [19]. Gonzalez-Cortes *et al.* stated that adding PEG to the impregnation solution can increase the distribution of active metals [19]. PEG is a template that wraps the particles so that no further aggregates form on the metal [20]. Behnejad *et al.* reported that the acquisition of PEG to synthesize NiMo/γ-Al_2O_3 revealed a lowering in sulfur content in a diesel by 12.4 ppm with a conversion of 90.1% at 350 ℃ [21]. Zhang *et al.* also wrote that the NiMo/γ-Al_2O_3 catalyst with the obtainment of PEG reduces sulfur levels in diesel up to 18.6 ppm with a conversion of 98.2% at 350 ℃ [22]. On the other hand, Simatupang *et al.* explained that citric acid could increase metal dispersion because it acts as a chelating agent in an impregnation solution that binds metals and prevents particle agglomeration from the NiMo catalyst [23].

Commonly, the amount of molybdenum loaded on the support is about 8-15% (w/w). Meanwhile, the nickel promoter weighs around 1-5% (w/w) [24]. Zhao *et al.* in their research employing a metal catalyst concentration of 2.5% NiO and 10% MoO_3, had HDS ability with a conversion of 67.81% [25]. Therefore, the NiMo/γ-Al_2O_3 catalyst was synthesized in this work by employing the target metal's 3% NiO and 15% MoO_3. The NiMo/γ-Al_2O_3 catalyst with the target metal content is expected to have higher HDS activity. Then, the authors aimed to apply two additives, namely PEG and citric acid, to determine the PEG and CA concentration variation effect on the characteristics of the NiMo/γ-Al_2O_3 catalyst.

2. Materials and Methods

2.1 Materials

The materials used in this work include Diesel Light Cycle Gas Oil (LCGO), alumina (γ-Al_2O_3 from PT Pertamina), nickel nitrate hydrate $Ni(NO_3)_2.6H_2O$ (Sigma-Aldrich), molybdenum trioxide (MoO_3 Sigma-Aldrich), ammonia solution 25% (NH_4OH Pro Analys Merck), polyethylene glycol (PEG) BM 1000 (sigma--Aldrich), and Citric Acid (CA Pro-analys Merck).

2.2 Preparation of Catalyst

The NiMo impregnant solution for determining PEG and CA concentration variations

was made by dissolving PEG and CA in 10 mL of distilled water. The addition of PEG variations of 2%, 4%, and 6% (w/w), while CA of 1%, 2%, and 4% (w/w). Then 22.72 g (15%) of MoO_3 was added, followed by 90 mL of ammonia (NH_4OH) solution until dissolved. Then, 14.92 g (3%) of $Ni(NO_3)_2.6H_2O$ was added and stirred until homogeneous. The impregnated solution was observed for the solution stability for 7 days. The impregnant solution with a total volume of 100 mL was then impregnated with 30 g of γ-Al_2O_3. The impregnated γ-Al_2O_3 was dried at 120 °C for 2 hours and calcined at 450 °C for 3 hours [26]. The addition of PEG is marked as P, and the addition of CA is C. The sample code can be seen in Table 1.

The total required impregnation solution is obtained from the support mass, and the water pick-up (WPU) results:

$$V_{\text{total}} = WPU \times support\ mass \quad (1)$$

WPU is acquired by weighing 0.5 g of support (W_o) and then soaking it in water for 15 minutes. After that, it was dried and weighed as (W_t). Then it is calculated by the Equation (2):

$$WPU = \frac{W_t - W_o}{W_o} \quad (2)$$

2.3. Catalysts Characterizations

Catalysts were characterized to determine their physical properties, including crystallinity, using X-Ray Powder Diffraction (XRD) 7000 Maxima-X with Cu radiation at a voltage of 40 kV and a current of 25 mA with 2θ range of 5-90°. Analysis of the support and catalyst components was carried out using the X-Ray Fluorescence (XRF) Axios PANalytical. Analysis of surface area, pore volume and diameter were carried out using ASAP 2400.

2.4. Catalyst Activity Analysis

The catalyst activity test was carried out using the Micrometrics PID EFFI-Microactivity Reactor. The catalyst activity test was carried out in several stages [26]: preparation, catalyst activation, and hydrodesulfurization. At the time of preparation of the catalyst, the power reactor, pump, and scales are first turned on. Then, 1 g of catalyst was put into the reactor. The flow of N_2 and H_2 gas from the cylinder was opened earlier. The line and reactor were cleaned of oxygen, and the catalyst was dried by flowing N_2 gas. Furthermore, catalyst activation was carried out through a sulfidation process, namely by flowing H_2 gas and dimethyl disulfide solution (DMDS) in naphtha, which reacted to form H_2S gas, which flowed into the catalyst compartment. After that, the DMDS or naphtha feed stream was stopped and continued with the hydrodesulfurization process. Diesel feed was supplied with LHSV 1, pressure 35.2 bar, and temperature of 315, 330, and 345 ℃. Sampling was conducted every 8 hours when the obtained product was accommodated in a bottle in the liquid product. Then the product is analyzed for sulfur content.

2.5. Sulfur Content Analysis

Sulfur analysis was carried out using a MultiTek Total Nitrogen Total Sulfur Analyzer [27]. Previously, the instrument was heated for 2 hours to raise the temperature to 1000 ℃. When the instrument was ready, a blank injection of isooctane was performed. Then, the sample was put into a 25 μL syringe, and we removed bubbles trapped in the syringe up to 10 μL. Then, the sample was injected into the instrument. The test was taken out three times. Each test ran for 4 minutes until the results of the sulfur content analysis were obtained in ppm units.

Table 1. Catalysts code Note: P is PEG and C is citric acid

Additive Compound	Concentration (w/w)	Catalyst Code
Polyethylene glycol (PEG)	2	NiMo-P2/γ-Al_2O_3
	4	NiMo-P4/γ-Al_2O_3
	6	NiMo-P6/γ-Al_2O_3
Citric Acid	1	NiMo-C1/γ-Al_2O_3
	2	NiMo-C2/γ-Al_2O_3
	4	NiMo-C4/γ-Al_2O_3
PEG and CA	2 and 1	NiMo-P2C1/γ-Al_2O_3

2.6. Density Analysis

Product density analysis was carried out using the Automatic Density Meter instrument [28]. The Automatic Density Meter was turned on and cleaned for optimization using toluene, and the syringe was rinsed and filled with 3 mL of sample. After that, the syringe was attached to the tool and we pressed start on the monitor tool, and waited until the density reading was completed and the measurement outcomes were recorded.

2.7. Cetane Index Analysis

Cetane index analysis was performed using the Automatic Distillation Analyzer instrument [29]. The Automatic Distillation Analyzer instrument was prepared in advance. The glassware was cleaned and the condenser was used. Then 100 mL of the sample was poured into the distillation flask. Then the OptiDist Temperature Sensor was installed on the distillation flask and into the tool circuit. Next, the lever on the front of the tool was pressed to raise the base plate. After that, the reservoir was closed with red rubber, then clicked start on the monitor to start the test. After that we waited until the density reading is complete and the measurement outcomes are recorded.

3. Results and Discussion

3.1 Effect of PEG and CA Addition on NiMo/γ-Al_2O_3 Catalyst

Catalyst preparation was carried out using the dry impregnation method in which NiMo metal was the active component, and γ-Al_2O_3 was the support. The NiMo/γ-Al_2O_3 was synthesized by adding MoO_3 and $Ni(NO_3)_2.6H_2O$ with NH_4OH gradually until the solution was homogeneous. Adding NH_4OH drives the formation of ammonium heptamolybdate and ammonium nickel nitrate solution, as shown in Equations (3) and (4):

$$MoO_3 + NH_4OH \longrightarrow (NH_4)_6Mo_7O_{24} \quad (3)$$

$$Ni(NO_3)_2.6H_2O + 6NH_4OH \longrightarrow Ni(NH_3)_6^{2+}(NO_3)_2 + 12H_2O \quad (4)$$

The impregnation solution must be stable so that the active phase can penetrate the support appropriately. The absence of molybdenum sediments in the impregnation solution noticed the stability of the impregnation solution. In this work, the impregnation solution stability was observed for seven days. Based on consumption in the industry, it must be stable within seven days to be used. In addition, the NH_4OH used is hygroscopic, so if it were carried out for more than seven days, more NH_4OH would evaporate. The impregnation solution decreases pH, forming molybdenum precipitates [26]. The impregnation solution stability was recorded in Table 2.

The obtained impregnation solution in this work were homogen and no precipitate was formed for seven days (Table 2). It confirmed that all impregnation solution have good stability. This stability was influenced by PEG and citric acid that were added. PEG has sufficient chains so that the particles fill in the cracks in the PEG arrangement [30]. PEG is a stable compound that acts as a template that wraps the particles so that aggregates do not form on the metal and generate the solubility of the active substance in the impregnation solution increases [20]. PEG has reactive groups or lone electron pairs (PEB) on the oxygen atoms at both ends of its structure. Lone electron pairs bind metal ions to the catalyst, leading to Mo [31]. The reaction that ensues is shown in Figure 1.

Table 2. Observations of the impregnation solution on the NiMo/γ-Al_2O_3 catalyst

Catalyst	Results
NiMo/γ-Al_2O_3	Homogen and no precipitate on 7 days
NiMo-P2/γ-Al_2O_3	Homogen and no precipitate on 7 days
NiMo-P4/γ-Al_2O_3	Homogen and no precipitate on 7 days
NiMo-P6/γ-Al_2O_3	Homogen and no precipitate on 7 days
NiMo-C1/γ-Al_2O_3	Homogen and no precipitate on 7 days
NiMo-C2/γ-Al_2O_3	Homogen and no precipitate on 7 days
NiMo-C4/γ-Al_2O_3	Homogen and no precipitate on 7 days
NiMo-P2C1/γ-Al_2O_3	Homogen and no precipitate on 7 days

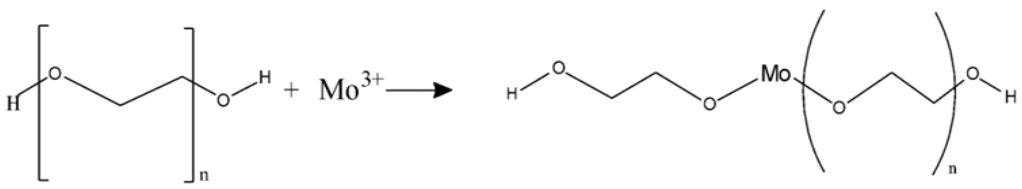

Figure 1. Reaction of PEG and Mo [32]

Meanwhile, citric acid (CA) is a tricarboxylic acid in which each molecule contains a carboxyl group and one hydroxyl group attached to a carbon atom and is widely utilized as a chelating compound in the synthesis of metal oxides [32]. Citric acid forms complexes depending on the metal. Francis *et al.* explained that citric acid forms bidentate complexes with Ni^{2+} metal [33]. The citric acid macromolecule's carboxylic group (-COOH) is deprotonated to release H^+ and citrate ions. The citrate ion strongly binds to Ni^{2+} metal [34]. The reaction that transpires is shown in Figure 2.

3.2 Characteristics of Catalysts

3.2.1 XRF Analysis

Analysis of active metal content in the catalyst was carried out using an XRF instrument. The catalyst's dispersion level can be seen from the amount of metal content in the catalyst. High metal content will reflect a satisfactory level of dispersion [35]. The catalyst's metal content outcomes can be seen in Table 3. Table 3 shows a comparison of PT. Pertamina's reference catalyst with the synthesized catalyst. The synthesized catalyst had a higher metal content than the reference catalyst. It indicates that PEG and CA effectively improve the dispersion of active metals on the catalyst support. Xiaodong Yi *et al.* [37] declared that adding PEG could raise the levels of active metals in the NiMo/γ-Al_2O_3 catalyst. Meanwhile, the effect of adding citric acid (CA) was explained by Mohanty [38], who said that CA dramatically influences the enlargement of metal oxides on the pore of the support surface by forming complex compounds.

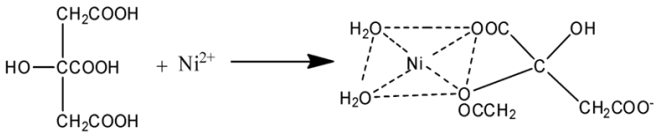

Figure 2. Reaction of citric acid (CA) and Ni^{2+} metal ion [36].

Table 3. XRF analysis results

Catalyst	NiO (%)	MoO_3 (%)
NiMo-P2/γ-Al_2O_3	3.12	13.51
NiMo-P4/γ-Al_2O_3	2.88	12.06
NiMo-P6/γ-Al_2O_3	2.93	12.38
NiMo-C1/γ-Al_2O_3	3.42	15.56
NiMo-C2/γ-Al_2O_3	3.33	14.67
NiMo-C4/γ-Al_2O_3	3.21	14.12
NiMo-P2C1/γ-Al_2O_3	3.19	13.98

Table 3 also exhibits the active metal content in the NiMo/γ-Al_2O_3 catalyst, which corresponds to 3% NiO and 15% MoO_3, and 1% CA. The metal content does not meet due to the uneven dispersion of Ni and Mo on the support. It causes a decrease in Mo metal content in the catalyst. Zhao *et al.* [25] conveyed that an impregnation solution that is not distributed evenly could cause agglomeration and reduce the active metal content of the catalyst. However, compared to the reference catalyst, the obtained catalyst in this work is distant and exceptional because it has a higher metal content. Thus, the catalyst's performance is potentially higher than the reference catalyst [25].

The determination of the best catalyst due to adding PEG and CA is chosen by the high active metal composition dispersed into the support. It is because the catalyst activity is closely related to the dispersion and distribution of the active phase on the support. The higher the dispersion of the active phase on the support, the higher the catalyst activity is obtained [24]. Table 3 showed that the highest metal composition was the addition of 2% PEG and 1% CA. Therefore, the catalyst was synthesized likewise by adding 2% PEG and 1% CA mixture in the impregnation solution. These additives were combined because PEG and CA have the valuable role of augmenting active metal dispersion and distribution and improving the HDS process. Zhang *et al.* synthesized a NiMo/γ-Al_2O_3 catalyst by adding PEG and a metal composition of 3.5% NiO and 12% MoO_3 with an HDS capability of 98.2% at 350 ℃ [22]. Mohanty [38] reported the NiMo/γ-Al_2O_3 catalyst, which was given the addition of CA with the active metal composition NiO 3% and 13% MoO_3 having an HDS ability of 83% at 370 ℃ [38]. Zhao *et al.* explained that catalysts without adding additives with a metal content of 2.5% NiO and 10% MoO_3 had an HDS capability of 67.81% [25].

The metal content in obtained NiMo-P2C1/γ-Al_2O_3 catalyst was close to the target, namely 3.19% and 13.98% for NiO and MoO_3, respectively (Table 3). Compared with the catalyst made early, the catalyst decreased in metal composition after adding a mixture of 2% PEG and 1% CA. PEG is a polymer with large molecular weight of 1000, increasing the viscosity of the impregnation solution, thus rendering a limited interaction space between metal ions and each added additive. In addition, it can also be influenced by the number of ligands present in a solution. In this case, there are ligands originating from PEG and CA. Ismangil & Hasanudin [39] expressed that metal cations

could bind to one or more functional groups to form chelate complexes. These functional groups can come from the same or different ligands [39]. If there is more than one ligand in a solution, the metal binding interaction by the functional groups of the ligand is hindered. It results in a lower distribution and dispersion than adding PEG and CA separately. However, the obtained catalyst in this work can still be used, because it is included in the range of NiO and MoO_3 catalysts loaded for the hydrotreating process. The MoO_3 composition loaded in the γ-Al_2O_3 support for the hydrotreating process ranges from 8-15% (w/w), while NiO ranges from 1-4% (w/w) [24]. If the dispersed MoO_3 metal is more than 15% (w/w), cracking occurs in the hydrotreating process. In contrast, the hydrogenation process is inhibited if the metal content is too low [40].

3.2.2 XRD Pattern of Catalysts

The NiMo/γ-Al_2O_3 catalyst was characterized using an XRD instrument to determine the catalyst phase. The catalyst diffractogram is used to detect the presence of MoO_3 crystal in the catalyst. MoO_3 crystals form if the distribution on the support is uneven. These crystals are disfavored because they are inactive. If the catalyst contains MoO_3 crystals, the active phase formed after the sulfidation process declines [41].

Figure 3 shows the diffraction pattern of the reference NiMo/γ-Al_2O_3 catalyst and the obtained catalyst in this work. Both the reference catalyst and obtained catalyst with PEG (2%, 4%, and 6%) have a similar diffraction pattern of γ-Al_2O_3 based on ICDD no. 98-009-9836 that is at 2θ: 36.97°; 46.11° and 66.70°. It shows that the impregnated γ-Al_2O_3 support remained in the γ-Al_2O_3 form. It confirmed that Ni and Mo species are spread evenly in the support pores because no NiO nor MoO_3 peaks appear in the diffraction pattern. Adding PEG can block metal aggregation and increase Mo dispersion [20].

Figure 3 displays the diffraction pattern of the NiMo/γ-Al_2O_3 with the addition of CA (1% and 4%) has a distinctive peak identical to the alumina spectrum based on ICDD no. 98-009-9836 that is at 2θ: 36.97°, 46.11°, and 66.70°. However, the NiMo/γ-Al_2O_3 catalyst with 2% CA exhibits peaks of MoO_3 which appear at 27.3°. Debecker *et al.* suggested that there was a diffraction peak at 2θ: 12.8°, 23.3°, 25.7°, 27.3°, and 33.7° are evidence for the presence of MoO_3 crystals [42]. The formation of MoO_3 crystals is due to the uneven distribution of Mo on the support surface [8,41].

Figure 4 shows the NiMo/γ-Al_2O_3 catalyst has an identical XRD spectrum with γ-Al_2O_3 based on ICDD no. 98-009-9836 that is at 2θ: 36.97°; 46.11° and 66.70°. It confirmed that the impregnated γ-Al_2O_3 support remained in the same γ-Al_2O_3 form as the prior addition of PEG and CA. Therefore, this catalyst is used for the further hydrodesulfurization process.

3.3 Surface Area of Catalysts

The active surface of the catalyst is an important parameter in characterizing the pore material and the surface of the catalyst. The surface area, pore volume, and pore size of catalysts were measured using a surface area analyzer and are shown in Table 4. Table 4 demonstrates the differences in surface area, pore volume, and pore diameter of the catalyst due to the acquisition of PEG and CA. The reference catalyst has a larger surface area than the catalyst with the addition of PEG and CA. Based on the active metal content of the catalyst

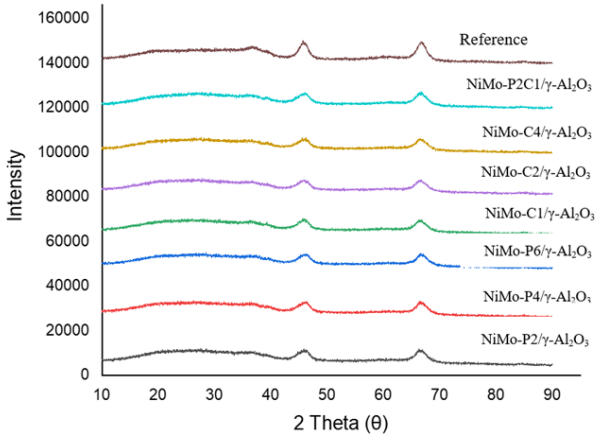

Figure 3. Diffraction pattern of NiMo/γ-Al_2O_3 catalyst

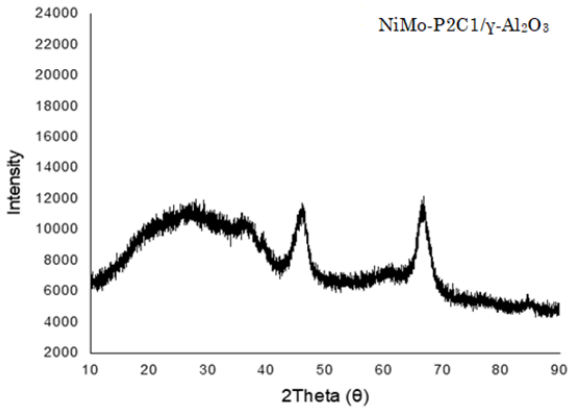

Figure 4. Diffraction pattern of NiMo/γ-Al_2O_3 with addition of PEG 2% and CA1% (NiMo-P2C1/γ-Al_2O_3)

(Table 3), the catalyst with the addition of PEG and CA has a higher metal content. It indicates that the Mo metal is well dispersed into the pore support, causing a reduced surface area [43]. Okamoto *et al.* stated that the surface area of the catalyst for the hydrotreating process is at least 150 m^2/g so that the catalyst, with the addition of PEG and CA, can still be employed for the hydrotreating process [40].

In contrast, the pore volume and diameter of the catalyst with the addition of PEG and CA is larger than the reference catalyst. The high content of active metals in the catalyst can increase pore volume and diameter [44]. in addition, the calcination affects the pore size increasing. Kusworo *et al.* explained that calcination removes air, carbon, and other impurities trapped in the catalyst pores, increasing the pore diameter [45]. Calcination could affect the catalyst's structure and properties related to the catalytic activity. Calcination also increases the active sites on the catalyst and lead to the probability of the reactants interacting with the surface of the catalyst increasing [46]. A large pore diameter makes it more straightforward for reactants to diffuse into and out of the pore optimally [47].

3.4 Catalytic Activity of NiMo-P2C1/γ-Al_2O_3

The catalytic activity of catalyst was carried out to yield Ultra Low Sulfur Diesel (ULSD) products through the HDS process using a PID microreactor. Product sampling is accomplished every 8 hours. The product delivered from the HDS process was tested for its physical characteristics by analyzing total sulfur, density, and cetane index values. Sulfur content analysis was carried out using the Multitek Total Sulfur Analyzer instrument. The total sulfur content of the obtained product of HDS is presented in Figure 5.

Figure 5 illustrates a relationship between HDS activity and operating temperature on the NiMo/γ-Al_2O_3 catalyst. There was a lowering in sulfur content in diesel after the HDS process was assumed out under constant pressure of 35.2 bar and LHSV of 1 h^{-1}. Figure 5 also demonstrates the hydrodesulfurization activity with sulfur content values at each temperature of 29.47 ppm, 16.94 ppm, and 9.55 ppm, respectively. The conversion of HDS was 96.10%, 97.80%, and 98.75%, respectively. It reveals that the higher temperature decreased the sulfur content. Abid *et al.* explained that the higher the reaction temperature, the more hydrodesulfurization activity increased [48]. The higher temperature triggers an increase in the rate of reaction. It was attributed to energy availability being more remarkable for the contact of the reactant molecules. This contact forces the number of collisions of the reactants on the catalyst's surface to increase, and the reaction of breaking the double bond and removing sulfur has become faster [13].

In this work, the sulfur content in diesel from the HDS process at 345 ℃ satisfied the specifications for diesel according to the Directorate General of Oil and Gas and Euro V with sulfur content in diesel of 9.55 ppm. The sulfur content obtained from this work was better

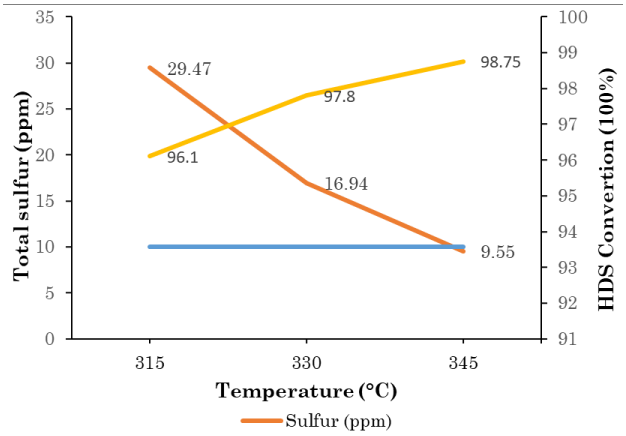

Figure 5. Hydrodesulfurization (HDS) activity

Table 4. The surface area, pore volume, and pore size of catalysts

Catalyst	Surface Area (m^2/g)	Pore Volume (cm^3/g)	Pore Size (Å)
Reference catalyst	223.07	0.40	72.72
NiMo-P2/γ-Al_2O_3	185.14	0.51	110.03
NiMo-P4/γ-Al_2O_3	188.48	0.51	109.20
NiMo-P6/γ-Al_2O_3	189.09	0.52	110.02
NiMo-C1/γ-Al_2O_3	187.19	0.51	108.80
NiMo-C2/γ-Al_2O_3	187.04	0.51	108.42
NiMo-C4/γ-Al_2O_3	187.83	0.51	108.97
NiMo-P2C1/γY-Al_2O_3	181.65	0.50	110.51

than those carried out by Zhang *et al.* who synthesized the NiMo/γ-Al_2O_3 catalyst by adding PEG that produced a sulfur content of 18.6 ppm at 350 ℃ [22], and Mohanty which had an HDS activity of 83% at 370 ℃ with the addition of CA to the NiMo/γ-Al_2O_3 catalyst [38].

The hydrodesulfurization process takes place through 2 pathways. The first is the hydrogenation reaction pathway (HYD), in which the aromatic ring is hydrogenated first and then followed by breaking the C-S bond. The second is hydrogenolysis, or direct desulfurization (DDS). They broke the C-S bond without employing aromatic ring hydrogenation [11]. The HDS reaction is shown in Figure 6. Adding PEG and CA to the impregnation of the catalyst effectively increases HDS activity, characterized by a significant decrease in sulfur content. Increased HDS is associated with high active metal dispersion because it leads to more active sites such as Ni-Mo-S [20]. Ni and Mo catalysts hold a specific role in the hydrodesulfurization process. The Mo metal plays to break the C-S bonds in thiophene. Meanwhile, Ni metal acts to cut the double bond in thiophene [49].

Density analysis was served to determine the value of density in diesel oil. In contrast, the cetane index is a rough ignition index and correlates with the cetane number or the time required to ignite in a specific space. The cetane index test aims to determine the density and composition of aromatic compounds in diesel fuel. The density and cetane index of diesel fuel were then compared with Indonesian regulatory standards and Euro V. The analysis results can be seen in Table 6. Table 6 shows that the density of diesel fuel in this work is lower than the standard according to both Indonesia and Euro V. The value of density value relatively decreases with increasing cetane index. It is because LCGO is a component of light diesel fraction which is usually used to blend with other types of of diesel with heavier fractions, such as Heavy Diesel Oil (HDO). Therefore, to get the density value according to the

Table 6. Results of product physical test analysis

Physical Test	Feed LCGO	Standard		Temperature (℃)	Analysis Result
		Indonesia	Euro V		
Density (g/mL)	0.8017	0.815-0.870	0.820-0.845	315	0.799
				330	0.797
				345	0.798
Cetane Index	50.3	Min. 45.0	Min. 46.0	315	52.4
				330	52.6
				345	53.6

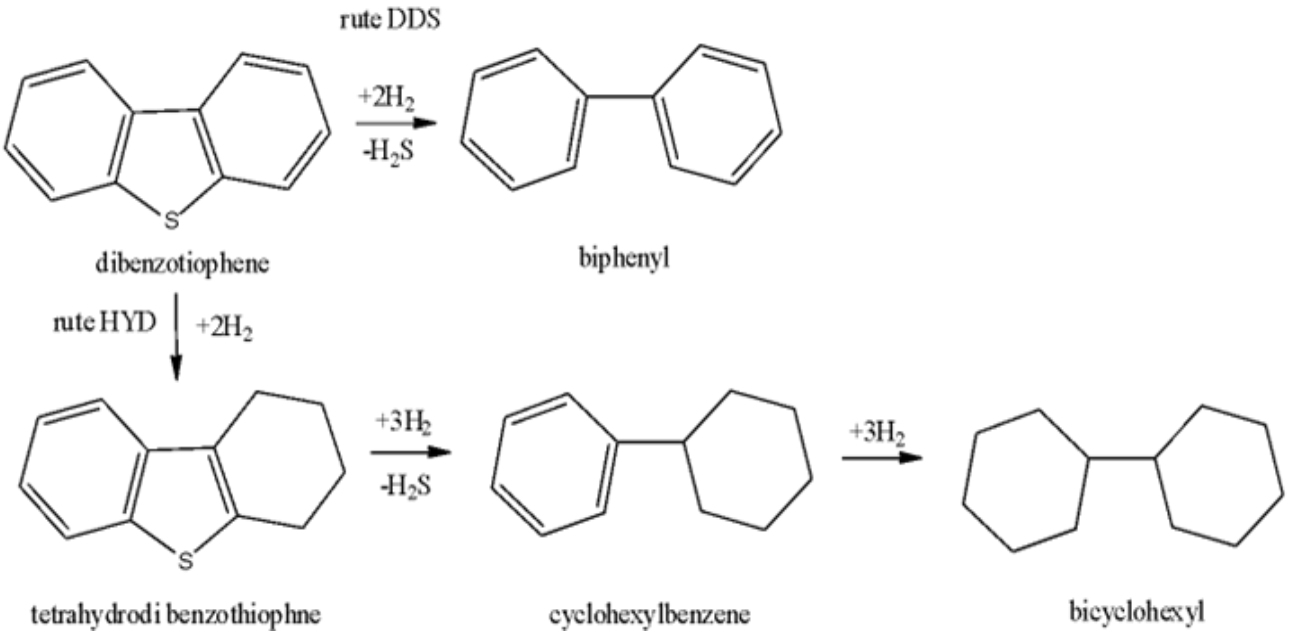

Figure 6. Hydrodesulfurization (HDS) reaction

standard, blending with other diesel components is required. Table 6 shows that the cetane index of diesel fuel is more significant than the standards at all temperatures. A high cetane index indicates the formation of a straight chain structure from more extended diesel or a change in the aromatic structure to a paraffin form (dearomatization) and a higher level of fuel saturation [50]. Knothe *et al.* explained that a fuel with a long straight chain has a higher cetane index [51].

In addition, the cetane index is strongly influenced by the composition of the Ni metal contained in the support. Higher Ni metal dispersion and distribution accelerate the breaking of the double bond in thiophene. Ni metal absorbs the double bond in thiophene, making it more effortless for the double bond to break [49]. It ensures that adding PEG and CA to the NiMo/γ-Al_2O_3 catalyst effectively increases hydrogenation, as indicated by the increased cetane index.

4. Conclusion

The best NiMo/γ-Al_2O_3 catalyst was obtained by impregnation of γ-Al_2O_3 support with the addition of 2% PEG and 1% CA. The XRF analysis showed that the active metal compositions were NiO 3.12% and MoO_3 13.51%. This catalyst reduced the sulfur content of diesel fuel to 9.55 ppm with an HDS conversion of 98.75% and high cetane index of 50.3.

Acknowledgements

The author would like to thank PT. Pertamina (Persero) to facilitate this research. The authors also thank Fuady Hanief and Ariawan Darari, who have assisted in testing catalysts in the materials and catalysts laboratory.

CRediT Author Statement

D. Sukandar oversaw conceptualization, validation, resources, data curation, and writing, while L. Badriyah oversaw formal analysis, inquiry, and draft preparation. The writing was overseen by W. Rustyawan. A. Adawiah spoke on manuscript writing. All of the writers read through the manuscript and instantly authorized it for publication.

References

[1] Pertamina. (2018). *Spesifikasi Bahan Bakar*. Jakarta: Pertamina.

[2] Yunita, R.D., Kiswandono, A.A. (2017). Kajian indeks standar pencemar udara (ISPU) sulfur dioksida (SO_2) sebagai polutan udara pada tiga lokasi di kota Bandar Lampung. *Analit: Analytical and Environmental Chemistry*, 2(1), 1–11.

[3] Mukono. (2011). *Aspek Kesehatan Pencemaran Udara*, Cet.1. Surabaya: Airlangga University Press.

[4] Mangalik, Y. (2019). Pengaruh Penggunaan Bahan Bakar Solar dan Pertamina Dex Terhadap Gas Buang Pada Mesin Diesel Ford Escord 1.8. *Undergraduate Thesis*, Universitas Hasanuddin.

[5] Jeevanandam, P., Klabunde, K.J., Tetzler, S.H. (2005). Adsorption of thiophenes out of hydrocarbons using metal impregnated nanocrystalline aluminum oxide. *Microporous and Mesoporous Materials*, 79(13), 101–110. 2005, doi: 10.1016/j.micromeso.2004.10.029.

[6] Sano, Y., Sugahara, K., HoiI, K., Korai, Y., Mochida, I. (2005). Two-step adsorption process for deep desulfurization of diesel oil. *Fuel*, 84(7-8), 903–910. doi: 10.1016/j.fuel.2004.11.019.

[7] Lussia, A. (2009). Desulfurisasi minyak solar dengan menggunakan adsorben zeolit alam. *Journals of Indonesia Zeolites*, 8(1), 1-5.

[8] Lestrari, H.D., Subagjo, S., Makertihartha, I. (2006). Sintesis katalis NiMo untuk hydrotreating coker nafta. *Jurnal Teknik Kimia Indonesia*, 5(1), 365–373. doi: 10.5614/jtki.2006.5.1.5

[9] Shafi, R., Hutchings, G.J. (2000). Hydrodesulfurization of hindered dibenzothiophenes: an overview. *Catalysis Today*, 59(3-4), 423–442. doi: 10.1016/S0920-5861(00)00308-4.

[10] Ozkan, U.S., Ni, S., Zhang, L., Moctezuma, E. (1994). Simultaneous hydrodesulfurization and hydrodenitrogenation of model compounds over Ni-Mo/γ-Al_2O_3 Catalysts. *Energy & Fuels*, 8(1), 249–257. doi: 10.1021/ef00043a039.

[11] Martínez, M.T., Benito, A.M., Callejas, M.A., Trasobares, S. (1998). Kinetics of sulfur removal from a liquid coal residue in thermal, hydrothermal, and hydrocatalytic cracking. *Energy & Fuels*, 12(2), 365–370. doi: 10.1021/ef970138b.

[12] Absi-Halabi, M. (1998). Performance comparison of alumina-supported Ni-Mo, Ni-W and Ni-Mo-W catalysts in hydrotreating vacuum residue. *Fuel*, 77(7), 787–790. doi: 10.1016/S0016-2361(97)00228-7.

[13] Steiner. (2002). *Kinetic and Deactivation Studies of Hydrodesulfurization Catalysts*. The Norwegian University of Science and Technology.

[14] Shyamal, K., Maity, S.K., Turaga, U.T. (2004). Search for an efficient 4,6-DMDBT hydrodesulfurization catalyst: a review of recent studies. *Energy & Fuels*, 18(5), 1227–1237. doi: 10.1021/ef030179+

[15] Topsøe, H., Hinnemann, B., Nørskov, J.K., Lauritsen, J.V., Besenbacher, F., Hansen, P.L., Hytoft, G., Egeberg, R.G., Knudsen, K.G. (2005). The role of reaction pathways and support interactions in the development of high activity hydrotreating catalysts. *Catalysis Today*, 107–108(12–22). doi: 10.1016/j.cattod.2005.07.165.

[16] Kamalia, F. (2018). Sintesis Katalis NiMo/γ-Al_2O_3, CoMo/γ-Al_2O_3, dan CoNiMo/γ-Al_2O_3 untuk Hidrodesulfurisasi Kerosin. *Undergraduate Thesis*, UIN Syarif Hidayatullah Jakarta.

[17] Li, H., Chu, H., Ma, X., Wang, G., Liu, F., Guo, M., Lu, W., Zhou, S., Yu, M. (2021). Efficient heterogeneous acid synthesis and stability enhancement of UiO-66 impregnated with ammonium sulfate for biodiesel production. *Chemical Engineering Journal*, 408(127–277). doi: 10.1016/j.cej.2020.127277.

[18] Satterfield, C.N., *Heterogeneous Catalysis in Industrial Practice, 2nd Edition*. New York., 1991.

[19] González-Cortés, S.L., Qian, Y., Almegren, H.A., Xiao, T., Kuznetsov, V.L., Edwards, P.P. (2015). Citric acid-assisted synthesis of γ-alumina-supported high loading CoMo sulfide catalysts for the hydrodesulfurization (HDS) and hydrodenitrogenation (HDN) reactions. *Appl. Petrochem. Res.*, 5(3), 181–197. doi: 10.1007/s13203-015-0097-y.

[20] Iwamoto, R., Kagami, N., Sakoda, Y., Iino, A. (2005). Effect of polyethylene glycol addition on NiO-MoO_3/Al_2O_3 and NiO-MoO_3-P_2O_5/Al_2O_3 Hydrodesulfurization Catalyst. *Journal of the Japan Petroleum Institute*, 48(6), 351–357. doi: 10.1627/jpi.48.351.

[21] Behnejad, B., Abdouss, M., Tavasoli, A. (2019). Comparison of performance of Ni–Mo/γ-alumina catalyst in HDS and HDN reactions of main distillate fractions. *Pet. Sci.*, 16(3), 645–656. doi: 10.1007/s12182-019-0319-5.

[22] Zhang, M., Fan, J., Chi, K., Duan, A., Zhao, Z., Meng, X., Zhang, H. (2017). Synthesis, characterization, and catalytic performance of NiMo catalysts supported on different crystal alumina materials in the hydrodesulfurization of diesel. *Fuel Processing Technology*, 156(2017), 446–453, doi: 10.1016/j.fuproc.2016.10.007.

[23] Simatupang, M. Asri, L., Purwasasmita, B.S. (2015). Pengaruh penambahan kitosan dan asam sitrat terhadap pembentukan $LiMn_2O_4$ spinel menggunakan metode sol gel. *Jurnal Teknologi Bahan dan Barang Teknik*, 5(61-62). doi: 10.37209/jtbbt.v5i2.60

[24] Rinaldi, N., Subagjo, Makertiharta, I., Haerudin, H. (2008). Preparasi katalis nafta hidrotreating dengan fasa aktif Ni-Mo pada penyangga lempung berpilar. *Jurnal Teknik Kimia Indonesia*, 7(2), 761–773. doi: 10.5614/jtki.2008.7.2.1

[25] Zhao, R., Zeng, L., Liang, J., Liu, C. (2016). Interaction between Ni promoter and Al_2O_3 support and its effect on the performance of NiMo/γ-Al_2O_3 catalyst in hydrodesulphurization. *Journal of Fuel Chemistry and Technology*, 44(5), 564–569. doi: 10.1016/S1872-5813(16)30026-3.

[26] Pertamina. (2015). *Katalis - Dasar Teori & Metoda Uji*. Jakarta: Pertamina.

[27] ASTM D5453. (2019). Standard Test Method for Determination of Total Sulfur in Light Hydrocarbons, Spark Ignition Engine Fuel, Diesel Engine Fuel, and Engine Oil by Ultraviolet Fluorescence.

[28] ASTM D4052. (2019). Standard Test Method for Density, Relative Density, and API Gravity of Liquids by Digital Density Meter.

[29] ASTM D86. (2019). Standard Test Method for Distillation of Petroleum Products and Liquid Fuels at Atmospheric Pressure.

[30] Rosmelina, L. (2012). Preparasi dan Karakterisasi Katalis Nanopartikel NiMo/Al_2O_3 dengan Metode Simple Heating untuk Sintesis Renewable Diesel,. Jakarta, FT UI.

[31] Sari, N., Kahraman, E., Sari, B., Özgün, A. (2006). Synthesis of Some polymer–metal complexes and elucidation of their structures. *Journal of Macromolecular Science, Part A*, 43(8), 1227–1235. doi: 10.1080/10601320600737484.

[32] Wang, X., Chen, X., Gao, L., Zheng, H., Ji, M., Shen, T., Zhang, Z. (2003). Citric acid-assisted sol–gel synthesis of nanocrystalline $LiMn_2O_4$ spinel as cathode material. *J. Cryst. Growth*, 256 (1–2), 123–127. doi: 10.1016/S0022-0248(03)01289-2.

[33] Francis, A.J., Dodge, C.J., Gillow, J.B. (1992). Biodegradation of metal citrate complexes and implications for toxic-metal mobility. *Nature*, 356(6365), 140–142. doi: 10.1038/356140a0.

[34] Li, Q., Chai, L., Wang, Q., Yang, Z., Yan, H., Wang, Y. (2010). Fast esterification of spent grain for enhanced heavy metal ions adsorption. *Bioresour. Technol.*, 101(10), 3796–3799. doi: 10.1016/j.biortech.2010.01.003.

[35] Francis, A.J., Dodge, C.J., Gillow, J.B. (1992). Biodegradation of metal citrate complexes and implications for toxic metal mobility. *Nature*, 356, 140-142. doi: 10.1038/356140a0

[36] Nugrahaningtyas, K.D., Trisunaryanti, W., Maruto, D., Yusnani, A. (2009). Preparation and characterization the non-sulfided metal catalyst: Ni/USY and NiMo/USY. *Indo. J. Chem.*, 9 (2), 177–183. doi: 10.22146/ijc.21526.

[37] Xiaodong.Yi, Guo, D., Li, P., Lian, X., Xu, Y., Dong, Y., Lai, W., Fang, W. (2017). One Pot Synthesis of NiMo-Al_2O_3 Catalysts by Solvent Free Solid State Method for Hydrodesulfurization. *RSC Advances*, 7, 54468–54474. doi: 10.1039/C7RA11892A

[38] Mohanty, S. (2011). Effect of Citric acid on Hydrotreating Activity of NiMo Catalysts, *Master Thesis*. University of Saskatchewan.

[39] Ismangil, Hasanudin, E. (2005). Degradasi mineral batuan oleh asam-asam organik. *Jurnal Ilmu Tanah dan Lingkungan*, 5(1), 1–17.

[40] Okamoto, Y., Arima, Y., Nakai, K., Umeno, S., Katada, N., Yoshida, H., Tanaka, T., Yamada, M., Akai, Y., Segawa, K., Nishijima, A., Matsumoto, H., Niwa, M., Uchijima, T. (1998). A study on the preparation of supported metal oxide catalysts using JRC-reference catalysts. I. Preparation of a molybdena–alumina catalyst. Part 1. Surface area of alumina. *Appl. Catal. A Gen.*, 170(2), 315–328. doi: 10.1016/S0926-860X(98)00064-7.

[41] Ulfah, M., Subagjo, S. (2012). Pengaruh perbedaan sifat penyangga alumina terhadap sifat katalis hydrotreating berbasis nikel-molibdenum. *Reaktor*, 14 (2), 151-157, doi: 10.14710/reaktor.14.2.151-157

[42] Debecker, D.P., Schimmoeller, B., Stoyanova, M., Poleunis, C., Bertrand, P., Rodemerck, U., Gaigneaux, U.M. (2011). Flame-made MoO_3/SiO_2–Al_2O_3 metathesis catalysts with highly dispersed and highly active molybdate species. *J. Catal.*, 277(2), 154–163. doi: 10.1016/j.jcat.2010.11.003.

[43] Rianto, L.B., Amalia, S., Khalifah, S.N. (2012). Pengaruh impregnasi logam titanium pada zeolit alam malang terhadap luas permukaan zeolit. *Alchemy Journal of Chemistry*, 2(1), 58-67, doi: 10.18860/al.v0i0.2295

[44] Efiyanti, L., Santi, D. (2016). Pengaruh Katalis NiO dan NiMoO terhadap perengkahan minyak cangkang biji jambu mete. *Jurnal Penelitian Hasil Hutan*, 34(3), 189-197, doi: 10.20886/jphh.2016.34.3

[45] Kusworo, T.D., Yusufina, D., Atyaforsa. (2013). Pengaruh katalis Co dan Fe terhadap karakteristik carbon nanotubes dari gas asetilena dengan menggunakan proses catalytic chemical vapour deposition (CCVD). *Reaktor*, 14(3), 234–241. doi: 10.14710/reaktor.14.3.234-241

[46] Tee, J.C., Aziz, M., Ismail, A.F., Rusop, M., Soga, T. (2009). Effect of reaction temperature and flow rate of precursor on formation of multi-walled carbon nanotubes. in *AIP Conference Proceedings*, 214–218. doi: 10.1063/1.3160133.

[47] Rahma, A. (2019). Sintesis dan Karakterisasi Katalis NiMo/γ-Al_2O_3 dengan Penambahan Zeolit HY, Zeolit Hirarki dan Silika, *Undergraduate Thesis*, UIN Syarif Hidayatullah Jakarta.

[48] Abid, M.F., Ahmed, S.M., Abu, H.W.H., Ali, S.M. (2019). Study on novel scheme for hydrodesulfurization of middle distillates using different types of catalyst, *Journal of King Saud University - Engineering Sciences*, 31(2), 144–151. doi: 10.1016/j.jksues.2017.11.006.

[49] Nugrahaningtyas, K.D. Pratiwi, N., Heraldy, E. (2018). Desulfurisasi katalitik tiofen menggunakan katalis CoMo/USY dalam reaktor batch. *ALCHEMY Jurnal Penelitian Kimia*, 14(1), 119–130. doi: 10.20961/alchemy.14.1.2368.119-130

[50] Jing, G. (2011). *Effects of Biodiesel Blending on Exhaust Emissions. PhD Thesis*. University of Kansas.

[51] Knothe, G., Matheaus, A.C., Ryan, T.W. (2003). Cetane numbers of branched and straight-chain fatty esters determined in an ignition quality tester. *Fuel*, 82(8), 971–975. doi: 10.1016/S0016-2361(02)00382-4.

[52] Niemantsverdriet, J. W. (2007). *Spectroscopy in Catalysis: An Introduction, 2nd Edition.* Germany. Wiley-VCH